PBDTTPD for plastic solar cells *via* $Pd(PPh_3)_4$-catalyzed direct (hetero)arylation polymerization

G. Marzano,[a] F. Carulli,[b] F. Babudri, [a] A. Pellegrino,[c] R. Po, [c] S. Luzzati[b] and G. M. Farinola*[a]

[a]*Dipartimento di Chimica, Università degli Studi di Bari Aldo Moro, Via Orabona 4, 70125 Bari, Italy.*

[b]*Consiglio Nazionale delle Ricerche, CNR, Istituto per lo Studio delle Macromolecole, ISMAC, via Bassini 15, 20133 Milan, Italy*

[c]*Centro Ricerche per le Energie Rinnovabili e l'Ambiente, Istituto Eni Donegani, Eni SpA, Via Fauser 4, 28100 Novara, Italy*

Polymeric photovoltaics have attracted considerable academic and industrial interest over the last few years because of their unique features. However, they still suffer from some drawbacks which have prevented so far massive industrial production. These drawbacks include high costs related to the preparation of active materials and high toxicity of organo-tin compounds usually involved in synthetic routes. In this context, we report the synthesis of one of the most promising polymers for bulk heterojunction (BHJ) solar cells, PBDTTPD (poly[(benzo[1,2-*b*:4,5-*b'*]dithiophene)-*alt*-(4*H*-thieno[3,4-*c*]pyrrole-4,6(5*H*)-dione)]), *via* Direct (Hetero)Arylation Polymerization (DHAP) in the presence, for the first time, of a low-cost Pd-catalyst [$Pd(PPh_3)_4$]. The outcome of the polymerization process is discussed in comparison with the synthesis of the same polymer *via* the Stille polycondensation. The photovoltaic performances of the polymer synthesized *via* DHAP are compared with those of the same polymer obtained *via* the Stille coupling and a commercially available PBDTTPD. The polymer synthesized by $Pd(PPh_3)_4$-catalyzed DHAP blended with $PC_{71}BM$ exhibits a power conversion efficiency up to 5.3%, higher than that of the Stille reference polymer, and comparable with that of the commercially available PBDTTPD, under the same processing conditions. These results confirm the potential of DHAP as a convenient alternative for the synthesis of D–A copolymers for plastic solar cells.

Introduction

Organic photovoltaics have attracted enormous academic and industrial interest in the last few decades. The possibility of obtaining lightweight, flexible and coloured modules *via* easy printing production procedures makes this technology particularly attractive for both indoor and outdoor applications. Conjugated polymers have gained much attention as donor materials for bulk hetero-junction (BHJ) solar cells;[1,2] remarkable improvements in power conversion efficiencies (PCEs) of lab-scale BHJ devices (over 10%)[3,4] have been achieved in the last few years, especially using donor–acceptor (D–A) polymers, consisting of alternation of an electron-donor and an electron-accepting unit in the polymer backbone. This approach enables fine tuning of the opto-electronic properties of the final materials depending on the molecular structures of the monomers involved in the polymerization process.[5] Besides the positive features characterizing the BHJ technology, and

the very encouraging performances achieved, some critical aspects still need to be addressed to make this technology suitable for large-scale production. In particular, the continuous race to break the best current efficiency has led to the design and synthesis of sophisticated polymeric structures, while fewer research efforts have been directed towards materials with an acceptable trade-off between structural complexity and device performances, keeping in proper account the production costs of scalable processes.[1,2] Moreover, state-of-the-art clearly shows that the most performing copolymers are prepared *via* Stille polymerization, involving highly toxic arylstannanes as monomers and producing stoichiometric amounts of trialkyltin bromide. This explains why poly(3-hexyl)thiophene (P3HT), in spite of its lower performances compared to those of other D–A copolymers, still remains the material which better fulfils the scalability requirements. Recently, Direct (Hetero)Arylation Polymerization (DHAP) has emerged as an alternative synthetic method to conventional cross-coupling reactions involving organometallic reagents, for the synthesis of organic electronic materials.[6–8] Typically, DHAP involves a functionalized (hetero)arene bearing a leaving group (I, Br) and an un-substituted aromatic compound which undergoes C–H bond activation in the presence of a transition metal catalyst; the reaction also requires the presence of a base (*e.g.* inorganic carbonates) and a carboxylate ligand that assists the C–H bond activation step in the concerted metalation-deprotonation (CMD) pathway.[9] In principle, the DHAP protocol allows us to solve some important issues affecting the scale-up production of push–pull copolymers, especially the need for pre-functionalization of the monomers to obtain organometallic intermediates used in the polymerization reaction, the use of toxic compounds and the production of stoichiometric amounts of metal-containing wastes. However, this reaction still needs to be optimized as a polymerization protocol, both for generality of the experimental conditions and for the choice of the catalyst.

Here, we offer a contribution to the progress in this topic, reporting the synthesis of **PBDTTPD** (**P_{DHAP}**) (poly[(benzo[1,2-*b*:4,5-*b*′]dithiophene) -*alt*-(4*H*-thieno[3,4-*c*]pyrrole -4,6(5*H*)-dione)]) bearing branched 2-ethylhexyl and *n*-octyl chains on BDT and TPD units, respectively, *via* $Pd(PPh_3)_4$-catalysed direct arylation polycondensation. As recently reported,[2] **PBDTTPD** represents one of the most promising polymers in OPVs in terms of low "synthetic complexity" and high power conversion efficiency. To the best of our knowledge, only a few papers dealing with the synthesis of **PBDTTPD** *via* direct arylation were reported:[10–12] they are essentially focused on synthetic aspects involving the use of quite expensive palladium(II) catalysts [Herrmann–Beller and $PdCl_2(MeCN)_2$]. Moreover, no mention about the photovoltaic properties of **PBDTTPD** obtained *via* DHAP has been reported so far. We think that the use of a cheaper Pd(0) catalyst such as $Pd(PPh_3)_4$, that is less frequently adopted in DHAP processes, may represent a significant improvement of this synthetic approach, especially with the aim of further decreasing the production costs. In order to compare the DHAP methodology with the Stille cross-coupling reaction, which until now has been the synthetic way of choice for D–A conjugated copolymers, we have also prepared a **PBDTTPD** copolymer (**P_{STILLE}**) by this coupling reaction. Furthermore, we also used a commercially available **PBDTTPD** (**P_{COMM}**, M_n = 15 kDa, M_w = 45 kDa) for the sake of comparison. Under the same processing conditions, **P_{DHAP}** displayed power conversion efficiency up to 5.3%, which is higher than that of **P_{STILLE}** and comparable with that of the commercial reference **P_{COMM}**.

Results and discussion

DHAP *vs.* Stille polymerization for the synthesis of PBDTTPD

A model reaction involving monobromo-benzodithiophene (BDT-Br) **1** (0.5 mmol) and TPD **2** (0.1 mmol) was carried out according to Scheme 1 to test the effectiveness of $Pd(PPh_3)_4$ as a catalyst in the synthesis of **PBDTTPD** *via* a direct arylation process. The experimental conditions and the results are summarized in Table 1.

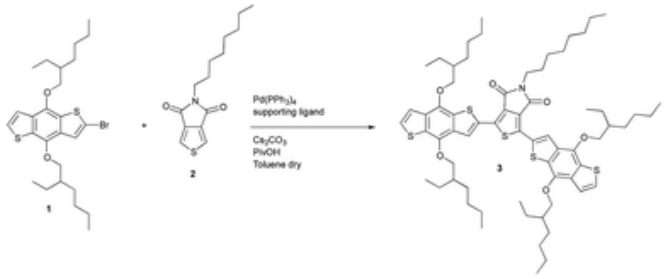

Scheme 1 *Model direct arylation reaction involving BDT-Br and TPD.*

Table 1 *Experimental conditions of model direct arylation reactions*[a]			
Entry	**Time**	**Supporting ligand**	**Yield**[b] **(%)**
1	24 h	P(*o*-OMePh)$_3$	86
2	24 h	—	51
a BDT-Br 1 (0.5 mmol), TPD 2 (0.1 mmol), P(*o*-OMePh)$_3$ (10% mol), PivOH (30% mol), Cs_2CO_3 (2 eq.), $Pd(PPh_3)_4$ (5% mol), and toluene dry (3 mL). **b** Isolated yield.			

Since tris(*o*-anisyl) phosphine [P(*o*-OMePh)$_3$] has been reported as an efficient supporting ligand for direct arylation reactions in nonpolar media,[13] the catalytic system consisting of $Pd(PPh_3)_4$ in combination with P(*o*-OMePh)$_3$ has been investigated (entry 1). The reaction was monitored by thin layer chromatography (TLC) using hexane/dichloromethane (volumetric ratio 1 : 1) as the eluent. After 24 hours, a solution color change from light yellow to dark red was observed. The crude product was purified by column chromatography obtaining **3** in 86% yield. In the absence of the supporting phosphine ligand (entry 2), the reaction still proceeds but it afforded the coupling product **3** in lower yield (51%). The compound **3** was fully characterized by $^1H/^{13}C$-NMR spectroscopy and high-resolution mass spectrometry (HR-MS); as shown in Fig. 1, its structure was easily elucidated considering some NMR resonances related to the starting products. In fact, the presence of the TPD unit is indicated by the typical ^1H resonance **a** (triplet at *ca.* 3.7 ppm) of the methylene protons bonded to nitrogen. The benzodithiophene (BDT) unit is characterized by (i) the terminal thienyl moiety which gives rise to two doublets **c** in the aromatic region (^3J = 5.5 Hz), whereas the substituted thienyl moiety gives a singlet **d** (this signal can be strongly deshielded in the presence of electron-withdrawing groups) and (ii) the OCH_2 protons **b** of the alkyl chains on the benzodithiophene unit in the 4.0–4.5 ppm range. According to these general considerations, the ^1H NMR spectrum of **3** confirmed the presence of BDT end

units (two doublets c at 7.38 and 7.43 ppm, respectively, ^3J = 5.5 Hz, and a singlet d at 8.68 ppm) and a central TPD unit (triplet a at *ca.* 3.7 ppm, ^3J = 7.5 Hz).

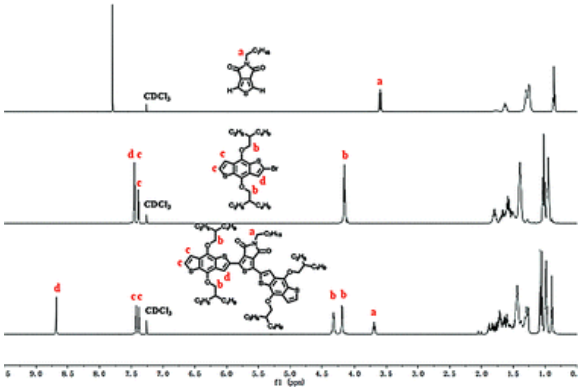

Figure 1 *^{1}H-NMR spectra (500 MHz, $CDCl_3$) of **1**, **2** and **3** involved in the model direct arylation reaction.*

Considering the positive outcomes of the model reaction combining $Pd(PPh_3)_4$ and [P(*o*-OMePh)$_3$] in toluene (Table 1, entry 1), we performed the polymerization process involving monomers **2** and **4** under the same experimental conditions as the model reaction. A reference polymer was also prepared *via* Stille cross-coupling (Scheme 2) by reacting monomers **5** and **6** (Scheme 2) in order to carry out a comparative study on the efficiency of the synthetic protocols and the performances in BHJ devices of the polymers synthesized. The experimental conditions adopted and the results obtained are reported in entries 1 and 2 of Table 2.

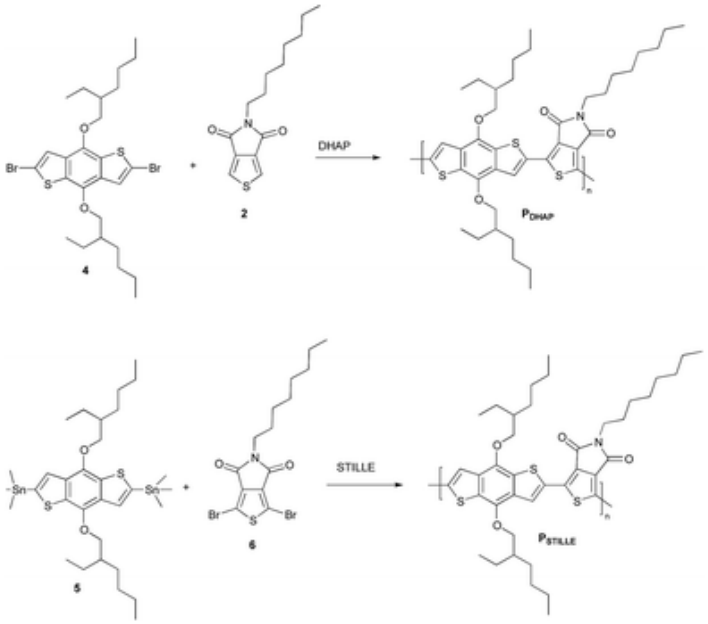

Scheme 2 *DHAP and Stille polymerization reactions for the synthesis of **PBDTTPD**.*

Table 2 *Experimental conditions of the polymerization reactions and characterization of the polymers obtained*

Entry	Polymer	Catalyst	Co-catalyst	Support ligand	Solvent	*T* (°C)	Yield[a] (%)	Molecular weight[b]	λ_{max}[c] (nm)	T_d[d] (°C)	Pd content[e] (mg kg^{-1})	Sn content[e] (mg kg^{-1})

								(kDa) M_w (M_n)				
	$\mathbf{P_{DHAP}}$[f]	$Pd(PPh_3)_4$	PivOH	P(*o*-OMePh)$_3$	Toluene	Reflux	80	72 (12)	553, 605, 634[g]	318	870 ± 10	—
2	$\mathbf{P_{STILLE}}$	$Pd_2(dba)_3$	—	P(*o*-MePh)$_3$	Toluene	Reflux	90	34 (10)	550, 595, 626[g]	310	420 ± 10	1410 ± 10

a *The products were obtained after Soxhlet extraction with $CHCl_3$ and reprecipitation from $CHCl_3$/MeOH.* ***b*** *Estimated by GPC in trichlorobenzene (TCB) at 100 °C calibrated on polystyrene standards.* ***c*** *Chlorobenzene solution UV-Vis absorption maxima.* ***d*** *Data derived from TGA.* ***e*** *Detected by ICP-MS after Soxhlet extractions and treatment with ammonia solution.* ***f*** *The reaction was conducted in the presence of Cs_2CO_3 (2 eq.) as the base.* ***g*** *Absorption peak related to the aggregated phase.*

Stille polymerization (entry 2, Table 2) was carried out following the standard protocol involving $Pd_2(dba)_3$/P(*o*-PhMe)$_3$ as the catalyst in refluxing toluene for 48 hours: under these conditions, the corresponding $\mathbf{P_{STILLE}}$ was obtained in 90% yield (M_n = 10 kDa and M_w = 34 kDa) after Soxhlet purification with $CHCl_3$. Similarly, the DHAP reaction (entry 1, Table 2) in the presence of $Pd(PPh_3)_4$/[P(*o*-OMePh)$_3$] proceeds smoothly showing a progressive color variation from light yellow to dark blue. After purification by Soxhlet extraction, the reaction afforded $\mathbf{P_{DHAP}}$ in good yield (80%) with a higher molecular weight (M_n = 12 kDa, M_w = 72 kDa) compared to the Stille reference polymer.

Characterization of the polymers synthesized and comparison with P_{COMM}

High-temperature NMR spectra of both Stille and DHAP polymers (see ESI†) acquired in $C_2D_2Cl_4$ at 90 °C confirmed that the two polymerization reactions lead essentially to the same macromolecular structure. TGA and DSC also corroborated the similarities between the two polymers; in particular, $\mathbf{P_{DHAP}}$ and the commercial reference $\mathbf{P_{COMM}}$ displayed a similar T_g value (102.4 °C and 103.4 °C, respectively) confirming the potentialities of the synthetic protocol reported herein.

Interestingly, UV-Vis absorption spectra recorded at room temperature in chlorobenzene solution of $\mathbf{P_{DHAP}}$, $\mathbf{P_{STILLE}}$ and $\mathbf{P_{COMM}}$ (Fig. 2a), respectively, displayed similar features. $\mathbf{P_{DHAP}}$ exhibits a bathochromic shift of its absorption profile compared to $\mathbf{P_{STILLE}}$ and $\mathbf{P_{COMM}}$; moreover, all polymers show an absorption peak between 626 and 634 nm that can be ascribed to aggregation phenomena occurring even in dilute solution. This aggregation peak is particularly pronounced for $\mathbf{P_{DHAP}}$. Temperature dependent UV-Vis absorption spectra in the range 25–85 °C (Fig. 2b–d), respectively, showed that the formation of aggregates was inhibited upon heating and the corresponding absorption peaks decreased accordingly. The increasing trend towards aggregation ($\mathbf{P_{DHAP}}$ > $\mathbf{P_{COMM}}$ > $\mathbf{P_{STILLE}}$) can be essentially explained by the M_w values of the polymers (72 kDa > 45 kDa > 34 kDa); moreover, since $\mathbf{P_{DHAP}}$ exhibits the highest polydispersity index, a pronounced aggregation peak could be explained by an important contribution from higher molecular weight chains on the solution behavior.

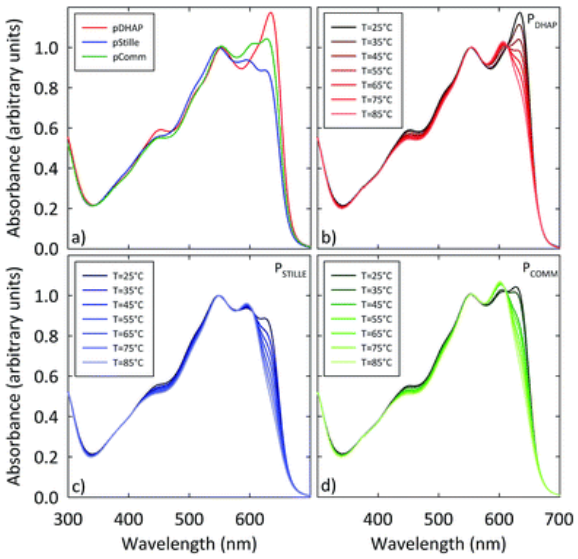

Figure 2 *Normalized UV-Vis absorption spectra of* ***PDHAP****,* ***PSTILLE*** *and* ***PCOMM*** *in chlorobenzene solution (0.2 mg mL^{-1}), (a) comparison of the absorption spectra at 25 °C and (b–d) temperature-dependent UV-Vis spectra of* ***PDHAP****,* ***PSTILLE*** *and* ***PCOMM****, respectively, in the range 25–85 °C.*

Photovoltaic performances

PDHAP, **PSTILLE** and **PCOMM** were tested, with [6,6]-phenyl-C_{71}-butyric acid methyl ester ($PC_{71}BM$), in bulk heterojunction devices with a standard architecture glass/ITO/PEDOT:PSS/**PBDTTPD**:$PC_{71}BM$/Ca/Al. The polymer : fullerene composition was 1 : 1.5 weight ratio and the active layer's thickness was kept around 70–80 nm, as a result of the device assembly optimization study. The device characteristics are summarized in Table 3. Cells were first investigated using chlorobenzene (CB) as the processing solvent. As a general trend we found that the CB devices exhibit the lowest performances, achieving the following power conversion efficiencies: 3.09% for the **PDHAP**, 2.70% for the **PSTILLE** and 3.3% for **PCOMM** based solar cells.

Table 3 *Photovoltaic parameters of solar cells through processing, based on* ***PSTILLE****,* ***PDHAP*** *and* ***PCOMM*** *blended with $PC_{71}BM$ (1 : 1.5 w/w)*[a]

PBDTTPD	Solvent	V_{oc} [V]	FF [—]	J_{sc} [mA cm^{-2}]	η[b] [%]
PSTILLE	CB	0.92 (0.93)	0.54 (0.54)	5.46 (5.57)	2.70% (2.80%)
	CB + 4% CN	0.89 (0.89)	0.55 (0.56)	7.82 (8.07)	3.82% (4.01%)
	CB + 4% CN*	0.93 (0.93)	0.57 (0.57)	8.82 (9.17)	4.65% (4.82%)
PCOMM	CB	0.91 (0.91)	0.54 (0.54)	6.88 (7.25)	3.37% (3.55%)
	CB + 4% CN	0.86 (0.87)	0.62 (0.62)	9.12 (9.63)	4.84% (5.02%)
	CB + 4% CN*	0.90 (0.92)	0.59 (0.63)	10.1 (10.2)	5.40% (5.71%)
PDHAP	CB	0.85 (0.86)	0.46 (0.48)	7.80 (7.86)	3.09% (3.27%)
	CB + 4% CN	0.77 (0.78)	0.35 (0.36)	8.84 (9.31)	2.39% (2.54%)
	CB + 4% CN*	0.92 (0.92)	0.55 (0.56)	10.07 (10.41)	5.14% (5.31%)

*a In brackets the best values obtained. * refers to active layers treated with ethanol after deposition. b Average PCE obtained from 12 devices.*

These efficiencies are considerably lower than the reference 5.5% efficiency that was reported in the literature for **PBDTTPD** with comparable molar mass to the polymers here under study.[14] It is worth noting that poor PV characteristics could arise from non-optimal blend morphology of the active layers prepared from CB. The addition of a small amount of 1-chloronaphthalene (CN) was reported to improve the performances of **PBDTTPD**:$PC_{71}BM$ solar cells[15,16] through the optimization of the blend morphology.[17] Therefore, we added a 4% vol of CN to the CB solution. In the three devices, we observed that CN processing induces a relevant enhancement of the J_{sc} and some reduction of the V_{oc}. The FF showed a slight enhancement upon CN processing for the $\mathbf{P_{STILLE}}$ and $\mathbf{P_{COMM}}$ devices. As a result, the efficiencies reached 3.82% for $\mathbf{P_{STILLE}}$ and 4.84% for $\mathbf{P_{COMM}}$ devices made from CB + CN. A different behavior was observed for $\mathbf{P_{DHAP}}$, where the FF decreased upon CN processing, thus limiting the efficiency to 2.39%. As shown in Fig. 3, for the $\mathbf{P_{DHAP}}$ device, the *J–V* curve showed a "kink" near the V_{oc} which is believed to be related to poor charge extraction.[18] Post-deposition surface treatment of the active layers with a polar solvent, ethanol (EtOH), was performed as a further processing step, since it was reported as a valuable method to engineer the active layer/electrode interfaces in BHJ solar cells.[19,20] Actually, upon EtOH treatment, the kink in the *J–V* curve of the $\mathbf{P_{DHAP}}$ cell disappeared. Accordingly, a simultaneous improvement of the FF, V_{oc} and J_{sc} parameters was observed leading to a two-fold enhancement of the power conversion efficiency of the $\mathbf{P_{DHAP}}$ cell up to 5.14% (see Table 3).

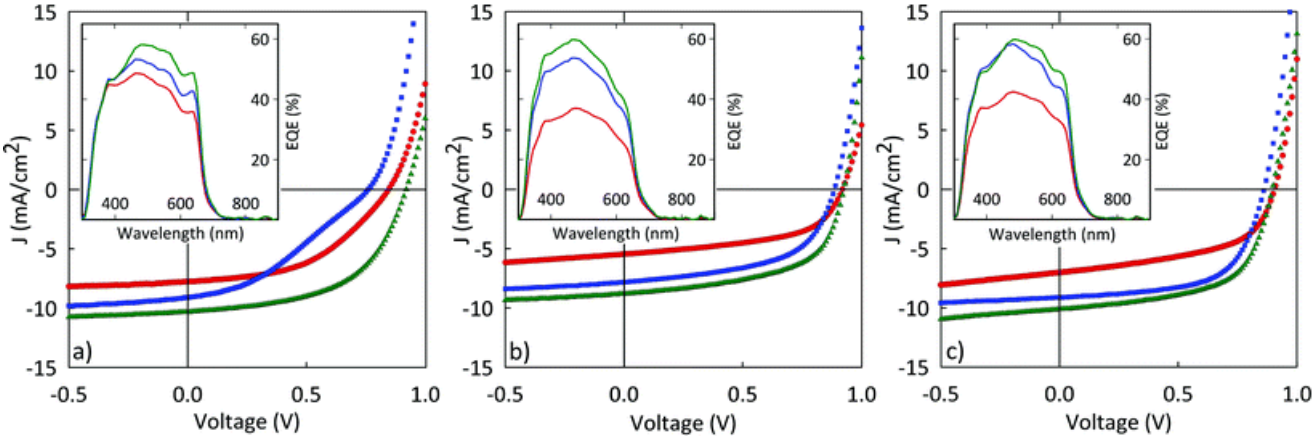

Figure 3 *J–V characteristics of solar cells based on polymer:$PC_{71}BM$ blends through processing with $\mathbf{P_{DHAP}}$ (a), $\mathbf{P_{STILLE}}$ (b) and $\mathbf{P_{COMM}}$ (c), respectively. Red curves (circles) represent blends cast from pure chlorobenzene, blue curves (squares) from chlorobenzene with 4% w/w of 1-chloronaphthalene and green curves (triangles) from chlorobenzene with 4% w/w of 1-chloronaphthalene treated with ethanol after deposition. In the insets, corresponding EQE spectra are shown.*

EtOH treatment also positively affected the performances of $\mathbf{P_{STILLE}}$ and $\mathbf{P_{COMM}}$ devices, which reached 4.65% for $\mathbf{P_{STILLE}}$ and 5.4% for $\mathbf{P_{COMM}}$ based devices. Therefore, the above findings demonstrate comparable photovoltaic performances for the three **PBDTTPD**s under study, which are in line with literature results for **PBDTTPD** with similar M_n.[14]

It is well known in the literature that metal impurities, which remain embedded in the polymers after the polymerization/purification process, can act as charge carrier traps negatively affecting the material performances in the corresponding solar cell devices.[21] In particular, a higher content of the residual palladium catalyst causes a higher density of trap states, which results in a decrease of the power conversion efficiencies. Therefore, inductively coupled plasma-mass spectrometry (ICP-MS) was used to detect residual palladium and tin contents (see ESI†). After Soxhlet extraction and subsequent polymer solution treatment with ammonia, 870 ppm and 420 ppm were found for **P$_{DHAP}$** and **P$_{STILLE}$**, respectively (Table 2). It is worth noting that, although **P$_{DHAP}$** showed a similar M_n value to **P$_{STILLE}$** but a significantly higher palladium content, it displayed higher power conversion efficiencies under the same processing conditions. In addition, although **P$_{COMM}$** showed palladium and tin contents much higher than our polymers (see ESI†), it shows the best PCE (see Table 3). These results pointed out that, in some cases, the level of metal-based impurities might not significantly affect the material performances in solar cells.

Recently, McGehee *et al.*[22] have reported that organic impurities (especially low molecular weight oligomers), which are difficult to remove by standard Soxhlet extraction from polymers with a high tendency to aggregate, can also play a critical role in both the performances and long-term stability of **PBDTTPD**-based solar cells. We think that, since **P$_{DHAP}$** has shown a strong tendency to aggregate, even in dilute solutions as confirmed by UV-Vis analysis (see Fig. 2), Soxhlet extractions might not be efficient for removing completely low molecular weight oligomers; the highest PDI value measured for **P$_{DHAP}$** corroborates our hypothesis. These organic impurities, as well as metal impurities, may affect the final efficiencies. However, polymer aggregation might also have an influence on the active blend morphology. McGehee *et al.* have recently reported that polymer aggregation in solution has a positive influence on the active layer blend morphology, which favors charge photogeneration in **PBDTTPD**-based devices.[17] It can be seen from Table 3 that the J_{sc} values of **P$_{DHAP}$** are relatively higher than those of both **P$_{STILLE}$** and **P$_{COMM}$** based devices. As discussed in the following, this feature is linked to the better capabilities of **P$_{DHAP}$** to form aggregates in solution (see Fig. 2 and relative discussion). The UV-Vis absorption spectra of the active layers for devices incorporating the three polymers are reported through processing in the ESI.† Upon CB deposition, the fingerprints of polymer aggregates are well evident in the spectra, being more pronounced in **P$_{DHAP}$**, decreasing in **P$_{COMM}$** and even more in **P$_{STILLE}$** active layers. Therefore, aggregate formation in the films is in agreement with the degree of aggregation of the polymer chains in solution. This indicates that the aggregates in solution can act as crystallization/aggregation seeds during the film forming process.[17] Upon CN processing, the absorption spectra evidence a further increase of the aggregated fraction in **P$_{STILLE}$** and **P$_{COMM}$**, while it is unchanged in the **P$_{DHAP}$** blend. Ethanol treatment does not substantially affect the UV-Vis spectral pattern. The EQE spectral patterns (see Fig. 3) change according to the UV-Vis spectra. Since the active layers show substantially similar O.D. max values and similar thicknesses, the absorption cross-sections are not substantially varying; therefore the changes of the EQE maxima values depicted in Fig. 3 and of the J_{sc} values of Table 3 evidence the differences of the exciton-to-electron efficiencies (IQEs). The photovoltaic characteristics of BHJs are strongly dependent on the blend morphology, directly responsible for charge photo-generation processes, such as

exciton dissociation and charge transport. Atomic force microscopy (AFM) was used to characterize the surface morphology of the active layers through processing, as shown in Fig. 4. Interestingly, there is a drastic change within the three polymer blends of the AFM morphologies upon CB deposition. The **P$_{STILLE}$** blend exhibits large micro-scale segregations. This type of pattern has been already observed in other polymer:$PC_{71}BM$ systems and has been ascribed to the formation of large PCBM-rich domains that limit the photon-to-electron conversion.[15,23] Going to **P$_{COMM}$**, the extension of these micro-domains is reduced, while in the **P$_{DHAP}$** active layer their presence is not detected. Upon CN processing, the formation of large domains has not been detected for all polymer samples. Therefore, in accordance with the recent literature,[17] the AFM morphology combined with the differences in polymer chain solvent aggregation could reasonably explain the observed trend of the J_{sc} for the three **PBDTTPD** polymer cells here under study.

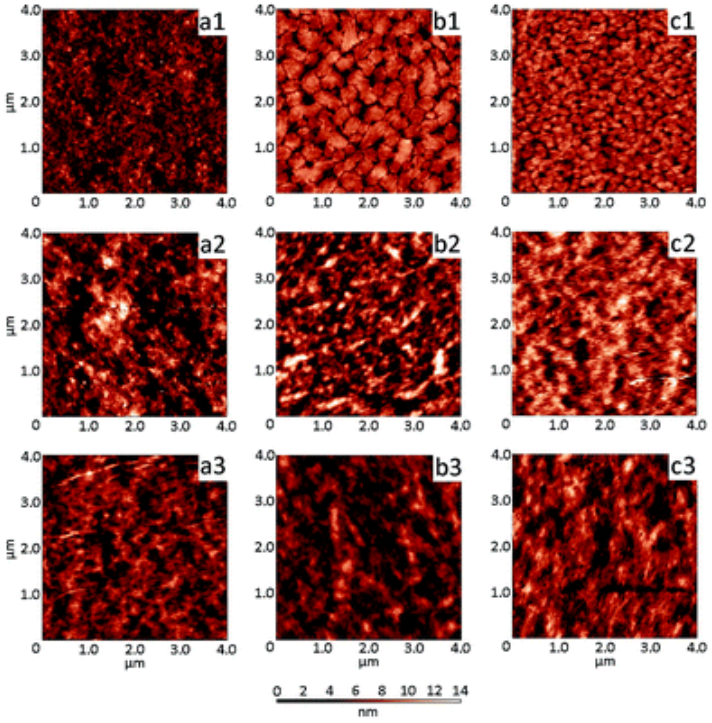

Figure 4 *AFM height images obtained in tapping mode of blends based on $PC_{71}BM$ with* ***P$_{DHAP}$*** *(a),* ***P$_{STILLE}$*** *(b) and* ***P$_{COMM}$*** *(c). Numerals 1, 2 and 3 refer to the blends cast from pure chlorobenzene, chlorobenzene with 4% w/w of 1-chloronaphthalene and chlorobenzene with 4% w/w of 1-chloronaphthalene and ethanol treatment after deposition, respectively.*

Conclusions

Palladium tetrakis(triphenylphosphine) $Pd(PPh_3)_4$ has been employed for the first time in the synthesis of **PBDTTPD***via* direct hetero(arylation) polymerization, replacing more expensive Pd catalysts. The photovoltaic performances of **PBDTTPD** obtained *via* DHAP have been measured in comparison with those of the polymers obtained *via* the Stille cross-coupling reaction, which currently represents the synthetic way of choice for the most performing D–A copolymers. Moreover, with the aim of gaining insight into the photovoltaic properties of the polymers synthesized, a commercially available **PBDTTPD** has been used as a

third term of comparison. Our comparative study revealed that the DHAP approach, under the appropriate experimental conditions, allows us to obtain better results than Stille coupling especially in terms of performances in solar cell devices of the final materials. The possibility of simplifying the synthetic protocol reducing, at the same time, the related costs for the preparation of the active material, undoubtedly makes this route particularly appealing in terms of scalability. Further investigations dealing with the use of our DHAP conditions for the synthesis of other TPD-based co-polymers are currently in progress.

Experimental section

Materials and methods

2-Bromo-4,8-bis((2-ethylhexyl)oxy)benzo[1,2-*b*:4,5-*b*′]dithiophene **1** was prepared according to a reported procedure[24] starting from the commercially available 4,8-bis((2-ethylhexyl)oxy)benzo[1,2-*b*:4,5-*b*′]dithiophene (Sunatech Inc). 5-Octyl-4*H*-thieno[3,4-*c*]pyrrole-4,6(5*H*)-dione **2**, 2,6-dibromo-4,8-bis((2-ethylhexyl)oxy)benzo[1,2-*b*:4,5-*b*′]dithiophene **4**, (4,8-bis((2-ethylhexyl)oxy)benzo[1,2-*b*:4,5-*b*′]dithiophene-2,6-diyl)bis(trimethylstannane) **5** and 1,3-dibromo-5-octyl-4*H*-thieno[3,4-*c*]pyrrole-4,6(5*H*)-dione **6** were purchased from Sunatech Inc. and used without further purification. Pivalic acid, cesium carbonate, tris(*o*-anisyl) phosphine [P(*o*-OMePh)$_3$], tri(*o*-tolyl)phosphine[P(*o*-MePh)$_3$], palladium-tetrakis(triphenylphosphine) Pd(PPh$_3$)$_4$ and tris(dibenzylideneacetone) dipalladium(0) Pd$_2$(dba)$_3$ were purchased from Sigma Aldrich and used without further purification. Toluene was distilled from sodium with benzophenone as an indicator under a nitrogen atmosphere.

^{13}C NMR spectra were acquired on a Varian INOVA 400 spectrometer at 100.61 MHz and ^{1}H NMR spectra were acquired on a Varian INOVA500 spectrometer at 500.13 MHz. Sample **3** was dissolved in $CDCl_3$ and the spectra were acquired at room temperature. The chemical shifts of ^{1}H and ^{13}C were reported relative to the residual chloroform signals at 7.26 and 77 ppm, respectively. *J* values are given in Hz. Poorly soluble polymers $\mathbf{P_{STILLE}}$ and $\mathbf{P_{DHAP}}$ were dissolved in $C_2D_2Cl_4$ (residual signal at 5.90 ppm) and the spectra were acquired at 90 °C. The high-resolution mass spectrum of **3** was acquired on a SHIMADZU high performance liquid chromatography-ion trap-time of flight mass spectrometer (LCMS-IT-TOF) *via* direct infusion of the sample using chloroform as the solvent. Gel permeation chromatography (GPC) analyses were performed with a Agilent 220 chromatograph equipped with a refractive index detector on 1,2,4-trichlorobenzene (TCB) solutions at 100 °C in order to overcome aggregation phenomena. Molecular weight calibration was carried out using polystyrene standards. GPC analysis of the commercially available $\mathbf{P_{COMM}}$ was performed under the same conditions of $\mathbf{P_{DHAP}}$ and $\mathbf{P_{STILLE}}$ in order to carry out a homogeneous comparison. ICP-MS analyses were performed on a Perkin-Elmer ICP-MS spectrometer (mod. Elan DRC-e) using ^{69}Ga as the internal standard; all samples were completely digested under microwave conditions in a Milestone Ethos One system using a mixture of HNO_3 : HCl (30/1) before submitting to ICP-MS analysis. UV-Vis spectra of the polymers were recorded on a SHIMADZU UV-2401PC. The thermal stability studies of polymers were carried out with a NETZSCH STA Jupiter F1 instrument, which allows Simultaneous Thermogravimetry-Differential Scanning

Calorimetry (STA/TG-DSC). Thermal analysis was performed heating about 10 mg of each polymer sample in an aluminum pan from 30 to 400 °C under a nitrogen atmosphere at a heating rate of 10 °C min^{-1}. The resulting plot includes the sample weight loss (% weight) *vs.* temperature and the μV mg^{-1} value related to the DSC measurement. Atomic force microscopy (AFM) investigations were performed using a NT-MDTNTEGRA apparatus in tapping mode under ambient conditions.

Procedure for the synthesis of 1,3-bis(4,8-bis((2-ethylhexyl)oxy)benzo[1,2-*b*:4,5-*b*′]dithiophen-2-yl)-5-octyl-4*H*-thieno[3,4-*c*]pyrrole-4,6(5*H*)-dione (3)

In a 10 mL Schlenk tube, monomer **1** (263 mg, 0.5 mmol), monomer **2** (27 mg, 0.1 mmol), cesium carbonate (65 mg, 0.2 mmol), pivalic acid (4 mg, 0.03 mmol), tris(*o*-anisyl) phosphine (3 mg, 0.01 mmol) and $Pd(PPh_3)_4$ (5 μmol, 6 mg) were added. The system was purged three times by vacuum/nitrogen cycles and anhydrous toluene (3 mL) was added. The reaction mixture was heated at reflux for 24 hours. The reaction was quenched by adding water. Then, the mixture was poured in a separatory funnel and extracted using dichloromethane three times. The organic phase was separated, dried over anhydrous sodium sulphate and filtered under vacuum. After the evaporation of the solvent, the crude product was purified by silica column chromatography (from hexane: dichloromethane = 1 : 1) to afford **3** (100 mg, 86%). δ_H (500 MHz, $CDCl_3$) 8.68 (2H, s), 7.43 (2H, d, J = 5.5), 7.38 (2H, d, J = 5.5), 4.36–4.28 (4H, m), 4.18 (4H, d, J = 5.5), 3.69 (2H, t, J = 7.5), 1.94–1.21 (48H, m), 1.07 (6H, t, J = 7.4), 1.05 (6H, t, J = 7.4), 0.99 (6H, t, J = 7.0), 0.98 (6H, t, J = 7.0), 0.89 (3H, t, J = 6.8). δ_C (100 MHz, $CDCl_3$) 162.4, 146, 144.1, 137.1, 133.1, 131.3, 131.1, 130.61, 130.57, 130, 127.2, 124.2, 120.4, 76.7, 76.2, 40.88, 40.84, 38.8, 31.99, 31.75, 30.65, 30.56, 29.9, 29.4, 29.39, 29.37, 28.6, 27.2, 24, 23.99, 23.33, 22.8, 14.39, 14.37, 14.28, 14.25, 11.54, 11.50. HR-MS: pred. value for $[M + Na]^+$ di $C_{66}H_{91}NO_6S_5$, 1176.5342, meas. 1176.5251.

Procedure for the synthesis of PBDTTPD*via* DHAP (P_{DHAP})

In a three-necked round-bottomed flask (25 mL), monomer **4** (500 mg, 0.83 mmol), monomer **2** (220 mg, 0.83 mmol), cesium carbonate (541 mg, 1.66 mmol), pivalic acid (26 mg, 0.25 mmol), tris(*o*-anisyl) phosphine (23 mg, 0.07 mmol) and $Pd(PPh_3)_4$ (48 mg, 0.04 mmol) were added. The system was purged three times by vacuum/nitrogen cycles and anhydrous toluene (8 mL) was added. The reaction mixture was heated at reflux for 48 hours. After this time, the polymer was end-capped by adding monomer **2** (220 mg, 0.83 mmol). The whole mixture was cooled to room temperature and poured in methanol. The solid product was washed with water, recovered by filtration and purified by Soxhlet extraction using methanol, acetone, hexane and chloroform, respectively. The solid residue was dissolved in chloroform (5 mg mL^{-1}) and an aqueous ammonia solution (NH_4OH) was added (volumetric ratio = 1 : 1). The mixture was refluxed for 5 hours under vigorous stirring and then it was cooled to room temperature. The organic phase was separated and concentrated and the polymer re-precipitated from methanol. A dark solid was recovered by filtration and dried under vacuum

at 60 °C to yield the target polymer (470 mg, 80%). δ_H (400 MHz, $C_2D_2Cl_4$, 90 °C) 9.13–7.87 (1H, br s), 4.88–3.17 (3H, br s), 2.49–0.31 (43H, br s).

Procedure for the synthesis of PBDTTPD*via* Stille polymerization (P_{STILLE})

In a three-necked round-bottomed flask (25 mL), monomer **5** (641 mg, 0.83 mmol), monomer **6** (351 mg, 0.83 mmol), tri(*o*-tolyl) phosphine (10 mg, 0.07 mmol) and $Pd_2(dba)_3$ (15 mg, 0.02 mmol) were added. The system was purged three times by vacuum/nitrogen cycles and anhydrous toluene (8 mL) was added. The reaction mixture was heated at reflux for 48 hours. After this time, iodobenzene (93 μL, 0.83 mmol) was added to the reaction mixture and reacted for 4 hours. To complete the end-capping procedure, 2-(tributylstannyl)thiophene (264 μL, 0.83 mmol) was added and reacted for 4 hours. The whole mixture was cooled to room temperature and poured in methanol. The solid product was recovered by filtration and purified by Soxhlet extraction using methanol, acetone, hexane and chloroform, respectively. The solid residue was dissolved in chloroform (5 mg mL^{-1}) and an aqueous ammonia solution (NH_4OH) was added (volumetric ratio = 1 : 1). The mixture was refluxed for 5 hours under vigorous stirring and then it was cooled to room temperature. The organic phase was separated and concentrated and the polymer re-precipitated from methanol. A dark solid was recovered by filtration and dried under vacuum at 60 °C to yield the target polymer (523 mg, 90%). δ_H (500 MHz, $C_2D_2Cl_4$, 90 °C) 9.20–7.92 (1H, br s), 4.97–3.22 (3H, br s), 2.46–0.32 (46H, br s).

Photovoltaic device fabrication and characterization

The devices were assembled with a standard geometry glass/ITO/PEDOT:PSS/active layer/cathode. Each ITO-glass substrate, Kintec 15 Ω sq^{-1}, was mechanically cleaned with wet paper and then washed in an ultrasonic bath at 55 °C, sequentially with water, acetone and isopropanol. Subsequently, the substrates were left in an isopropanol bath for 1 h. After drying under a compressed nitrogen flow, the substrates underwent 10 minutes of plasma treatment. Next, PEDOT:PSS (Clevios VP Al 4083) was spin coated at 2000 rpm for 60 seconds (40 nm thick) and dried in air on a 100 °C hot plate for 10 min. After annealing, the hot substrates were inserted into a glovebox where the device assembling was completed. The polymers and $PC_{71}BM$ (Solenne BV, 99% purity) were dissolved at the composition of 1 : 1.5 weight ratio in chlorobenzene (CB), with a solute concentration of 20 mg mL^{-1}. The solutions were stirred overnight at 85 °C, prior to spin coating deposition. Some active layers were prepared by adding 4% in volume of 1-chloronaphthalene (CN) to the CB solutions. The active layers were spin coated at 1800 rpm for 90 seconds: under these conditions film thicknesses were ~70 nm. Some samples underwent a further surface treatment with ethanol: 200 μL of ethanol were dropped on active layers 90 seconds after its deposition. Ethanol treated devices were subsequently spin coated at 2000 rpm per 60 seconds in order to remove the excess solvent. The films were left in a glovebox for 1 hour before the cathode evaporation. Finally, a 30 nm calcium layer and a 100 nm Al layer were thermally evaporated, through a shadow mask under a pressure of 2.10–6 mbar. The deposition rates were respectively 0.1 nm s^{-1} and 0.7 nm s^{-1} for Ca and Al. There were 6 devices on a single substrate and each with an active area of 6 mm^2. The current density–voltage measurements were performed directly in the glovebox where the

solar cells were assembled, with a Keithley 2602 source meter, under AM 1.5G solar simulation (ABET 2000). The incident power, measured with a calibrated photodiode (Si cell + KG5 filter), was 100 mW cm^2. The EQE spectral responses were recorded by dispersing a Xe lamp through a monochromator, using a Si solar cell with a calibrated spectral response to measure the incident light power intensity at each wavelength. The devices were taken outside the glovebox for the EQE measurements, after mounting them on a sealed cell to avoid moisture and oxygen exposure.

Acknowledgements

The authors would like to thank Dr Annalisa Congiu and Dr Sara Perucchini (Eni SpA) for ICP-MS analyses, as well as Dr Alessandra Tacca (Eni SpA), Dr Stefano Chiaberge (Eni SpA) and Dr Diego Antonioli (UniPO) for thermal analyses. We would also like to acknowledge Dr Sergio Matera for his important support during the initial steps of this work. MIUR with Università degli Studi di Bari Aldo Moro (Progetto PRIN2012 prot. 2012A4Z2RY and Progetto PON 02-00563-3316357 "Nanotecnologie Molecolari per la Salute dell'Uomo e l'Ambiente_MAAT"), Regione Puglia (APQ Reti di Laboratorio "Laboratorio Regionale di Sintesi e Caratterizzazione di Nuovi Materiali Organici e Nanostrutturati per Elettronica, Fotonica e Tecnologie Avanzate" Prog. Cod. 20) and Eni SpA are acknowledged for the financial support.

References

1. G. Marzano , C. V. Ciasca , F. Babudri , G. Bianchi , A. Pellegrino , R. Po and G. M. Farinola , *Eur. J. Org. Chem.*, 2014, **30** , 6583
2. R. Po , G. Bianchi , C. Carbonera and A. Pellegrino , *Macromolecules*, 2015, **48** , 453
3. J. You , L. Dou , K. Yoshimura , T. Kato , K. Ohya , T. Moriarty , K. Emery , C.-C. Chen , J. Gao , G. Li and Y. Yang , *Nat. Commun.*, 2015, **4** , 1446.
4. Y. Liu , J. Zhao , Z. Li , C. Mu , W. Ma , H. Hu , K. Jiang , H. Lin , H. Ade and H. Yan , *Nat. Commun.*, 2014, **5** , 5293.
5. Y.-J. Cheng , S.-H. Yang and C.-S. Hsu , *Chem. Rev.*, 2009, **109** , 5868.
6. G. L. Mercier and M. Leclerc , *Acc. Chem. Res.*, 2013, **46** , 1597.
7. K. Okamoto , J. Zhang , J. B. Housekeeper , S. R. Marder and C. K. Luscombe , *Macromolecules*, 2013, **46** , 8059.
8. G. Marzano , D. Kotowski , F. Babudri , R. Musio , A. Pellegrino , S. Luzzati , R. Po and G. M. Farinola , *Macromolecules*, 2015, **48** , 7039. J. Kuwabara , T. Yasuda , S. J. Choi , W. Lu , K. Yamazaki , S. Kagaya , L. Han and T. Kanbara , *Adv. Funct. Mater.*, 2014, **24** , 3226, S. Chen , K. C. Lee , Z.-G. Zhang , D. S. Kim , Y. Li and C. Yang , *Macromolecules*, 2016, **49** , 527, X. Wang , K. Wanga and M. Wang , *Polym. Chem.*, 2015, **6** , 1846, M. Gruber , S.-H. Jung , S. Schott , D. Venkateshvaran , A. J. Kronemeijer , J. W. Andreasen , C. R. McNeill , W. W. H. Wong , M. Shahid , M.

Heeney , J.-K. Lee and H. Sirringhaus , *Chem. Sci.*, 2015, **6** , 6949, S.-W. Chang , H. Waters , J. Kettle , Z.-R. Kuo , C.-H. Li , C.-Y. Yu and M. Horie , *Macromol. Rapid Commun.*, 2012, **33** , 1927.

9. S. I. Gorelsky *Coord. Chem. Rev.*, 2013, **257** , 153.
10. S. Beauprè , A. Pron , S. H. Drouin , A. Najari , L. G. Mercier , A. Robitaille and M. Leclerc , *Macromolecules*, 2012, **45** , 6906.
11. M. Wakioka , N. Ichihara , Y. Kitano and F. Ozawa , *Macromolecules*, 2014, **47** , 626.
12. T. L. D. Tam and T. T. Lin , *Macromolecules*, 2016, **49** , 1648.
13. X. Wang and M. Wang , *Polym. Chem.*, 2014, **5** , 5784.
14. Y. Zou , A. Najari , P. Berrouard , S. Beauprè , B. R. Aïch , Y. Tao and M. Leclerc , *J. Am. Chem. Soc.*, 2010, **132** , 5330.
15. C. Cabanetos , A. E. Labban , J. A. Bartelt , J. D. Douglas , W. R. Mateker , J. M. Frechét , M. D. McGehee and P. M. Beaujuge , *J. Am. Chem. Soc.*, 2013, **135** , 4656.
16. B. Friedel , T. J. K. Brenner , C. R. McNeill , U. Steiner and N. C. Greenham , *Org. Electron.*, 2011, **12** , 1973.
17. J. A. Bartelt , J. D. Douglas , W. R. Mateker , A. E. Labban , C. J. Tassone , M. F. Toney , J. M. Frechét , P. M. Beaujuge and M. D. McGehee , *Adv. Energy Mater.*, 2014, **4** , 1301733.
18. B. Qi and J. Wang , *Phys. Chem. Chem. Phys.*, 2013, **15** , 8972.
19. X. Liu , W. Wen and G. C. Bazan , *Adv. Mater.*, 2012, **4** , 4505.
20. Q. Wang , Y. Zhou , H. Zheng , J. Shi , C. Li , C. Q. Su , L. Wang , C. Luo , D. Hu , J. Pei , J. Wang , J. Peng and Y. Cao , *Org. Electron.*, 2011, **12** , 1858.
21. N. Camaioni , F. Tinti , L. Franco , M. Fabris , A. Toffoletti , M. Ruzzi , L. Montanari , L. Bonoldi , A. Pellegrino , A. Calabrese and R. Po , *Org. Electron.*, 2012, **13** , 550, F. C. Krebs , B. Nyberg and M. Jørgensen , *Chem. Mater.*, 2004, **16** , 1313, K. T. Nielsen , K. Bechgaard and F. C. Krebs , *Macromolecules*, 2005, **38** , 658, M. P. Nikiforov , B. Lai , W. Chen , S. Chen , R. D. Schaller , J. Strzalka , J. Maserb and S. B. Darling , *Energy Environ. Sci.*, 2013, **6** , 1513, J. H. Bannock , N. D. Treat , M. Chabinyc , N. Stingelin , M. Heeney and J. C. De Mello , *Sci. Rep.*, 2016, **6** , 23651, P. A. Troshin , D. K. Susarova , Y. L. Moskvin , I. E. Kuznetov , S. A. Ponomarenko , E. N. Myshkovskaya , K. A. Zakharcheva , A. A. Balakai , S. D. Babenko and V. F. Razumov , *Adv. Funct. Mater.*, 2010, **20** , 4351, O. Usluer , M. Abbas , G. Wantz , L. Vignau , L. Hirsch , E. Grana , C. Brochon , E. Cloutet and G. Hadziioannou , *ACS Macro Lett.*, 2014, **3** , 1134.
22. W. R. Mateker , J. D. Douglas , C. Cabanetos , I. T. Sachs-Quintana , J. A. Bartelt , E. T. Hoke , A. E. Labban , P. M. Beaujuge , J. M. J. Fréchet and M. D. McGehee , *Energy Environ. Sci.*, 2013, **6** , 2529..
23. C. V. Hoven , X.-D. Dang , R. C. Coffin , J. Peet , T.-Q. Nguyen and G. C. Bazan , *Adv. Energy Mater.*, 2010, **22** , E63.
24. M. Urbani , M. Medel , S. A. Kumar , M. Ince , A. N. Bhaskarwar , D. González-Rodriguez , M. Grätzel , M. K. Nazeeruddin and T. Torres , *Chem.–Eur. J.*, 2015, **21** , 16252.